

Transcriptomic insights into the molecular aspects of salt stress responses in *Kandelia candel* roots

Jianhong XING^{1,2} , Dezhuo PAN¹ , Lingxia WANG³ , Fanglin TAN⁴ , Wei CHEN^{1,*} 

¹College of Life Sciences, Fujian Agriculture and Forestry University, Fuzhou, Fujian, China

²College of Resources and Chemical Engineering, Sanming University, Sanming, Fujian, China

³College of Life Sciences, Ningxia University, Yinchuan, Ningxia, China

⁴Fujian Academy of Forestry Sciences, Fuzhou, Fujian, China

Received: 12.09.2019 • Accepted/Published Online: 10.02.2020 • Final Version: 17.03.2020

Abstract: The mangrove plant *Kandelia candel* is a type of woody halophyte that grows in tropical and subtropical ocean intertidal zones and exhibits a high salt tolerance. In this study, 61,970 unigenes were obtained from the roots of 60-day-old *K. candel* seedlings treated with 0 (control), 200, 400, and 600 mM NaCl for 3 days with an N50 of 1510 bp. Moreover, 454, 311, and 2663 genes were differentially expressed under 200, 400, and 600 mM NaCl treatments, respectively. These differentially expressed genes were primarily involved in plant hormone signal transduction, carbohydrate and energy metabolism, amino acid metabolism, stress response, and defense. The levels of 12 important differentially expressed genes were confirmed by qRT-PCR, showing that the changing trend was generally consistent with the results of the transcriptomic analysis. In addition, physiological parameters involved in energy metabolism, amino acid metabolism, and the reactive oxygen species scavenging process were significantly increased under salt stress treatment, and the trend was consistent with the results of transcription and qRT-PCR. This study indicated that *K. candel* roots could tolerate high salt stress by enhancing ethylene signal transduction, maintaining a stable energy supply, increasing antioxidant capacity. Specially, we found that accumulation of γ -aminobutyric acid and glutamate, but not proline, might play an important role in salt tolerance in the roots of *K. candel*.

Key words: *Kandelia candel*, transcriptome, salt tolerance, ethylene signal, energy metabolism

1. Introduction

In recent years, the problem of soil salinization has become increasingly prominent, which leads to the decline of land productivity and poses a major threat to the sustainable development of agriculture (Roy et al., 2014). It is worthwhile to investigate the salt tolerance mechanism of plants and identify salt-tolerant gene resources and address the intricate and serious problem of soil salinization.

So far, the molecular and physiological mechanisms of salt tolerance in plants have been demonstrated in model plants, which are primarily important crops and terrestrial herbaceous halophytes (Seki et al., 2002; Walia et al., 2007; Yao et al., 2011; Mishra and Tanna, 2017). Mangroves, woody salt-tolerant plants, grow in the intertidal coastal zone and are impregnated by seawater periodically. Such plants have developed a set of salt-tolerant mechanisms which differ from those of freshwater and terrestrial plants. Therefore, investigating the salt-tolerant mechanism of mangroves is desirable to achieve a better understanding of the salt-tolerant characteristics in woody plants, and

provide a theoretical basis and genetic resources for cultivating salt-tolerant crops.

A previous study revealed that the mangrove plant *Sonneratia alba* maintains the intracellular Na⁺/K⁺ balance by increasing the absorption of K⁺ (Yasumoto et al., 1999). The structural research of the root in the mangrove plant *Bruguiera gymnorrhiza* indicated that the plant could resist salt by accumulating special osmotic regulators (such as triterpenoid alcohols) in the cytoplasmic membrane to prevent the passage of salt ions, thereby avoiding the negative effects of salt (Miyama and Tada, 2008). *Laguncularia racemosa* can improve salt tolerance through the Na⁺ compartmentalization in the cells of its stems and leaves (Cram et al., 2002). With the development of high-throughput sequencing and bioinformatics analysis technologies, considerable effort has been performed to study the salt tolerance mechanism of mangrove plants in the perspective of omics. A microarray technique was used to analyze the expression pattern of the root genes in the mangrove plant *Ceriops tagal* under salt stress, and

* Correspondence: weichen909@163.com

59 differentially expressed genes (DEGs) were obtained (Liang et al., 2012). An oligoarray technique has been used to analyze the leaves of *B. gymnorrhiza* under salt stress, demonstrating that increasing the soluble sugar contents and maintaining the balance of Na^+ and K^+ in the cells play important roles in salt tolerance (Miyam et al., 2008). However, Illumina high-throughput sequencing technology provides a powerful tool to further understand the molecular mechanism of salt tolerance in mangrove plants at the genome and transcriptome levels. In recent years, high-throughput mRNA sequencing (RNA-Seq) has been used to analyze the transcriptome of mangrove plants, such as *Rhizophora apiculata*, *B. gymnorrhiza*, and *Carallia brachiata*. The results showed that the expression of stress-resistant genes may be the key factor to improve their ability to resist extreme environments (Guo et al., 2017). RNA-Seq analysis of the roots in the salt-secreting mangrove plant *Avicennia officinalis* under salt stress showed that the abscisic acid and ethylene-mediated phytohormone signaling pathways could play important roles in the response to salt stress (Krishnamurthy et al., 2017). These studies have provided a preliminary exploration to reveal the salt tolerance mechanism of mangrove plants at the transcriptome level. However, currently, there is no systematic and in-depth study on the molecular regulation mechanism of salt tolerance in the roots of nonsalt-secreting plants.

Kandelia candel (L.), a typical nonsalt-secreting mangrove plant, has formed a unique salt tolerance mechanism during a long evolutionary process that enables it to withstand up to 600 mM salt stress (Wang et al., 2015, 2016). Its salt tolerance is accomplished through the regulation of gene expression, which contains abundant salt-tolerant gene resources. Therefore, molecular analysis of the salt-tolerant mechanism of *K. candel* can provide new evidence to reveal the salt-tolerant mechanism of woody plants. In this study, the root transcriptome of *K. candel* seedlings treated with NaCl was sequenced and analyzed using an Illumina HiSeq 2000 platform, and the expression changes of DEGs were compared in more detail. Combined with qRT-PCR analysis and a physiological parameter assay, the salt-tolerant candidate genes related to metabolic pathways including plant hormone signal transduction, carbohydrate and energy metabolism, amino acid metabolism, stress responses, and defense were analyzed. Our study will thoroughly reveal the molecular regulation mechanism of the adaptation of *K. candel* to a high salinity environment.

2. Materials and methods

2.1. Materials and treatment

The hypocotyls of *K. candel* were collected from the Zhangjiangkou Mangrove Forestry National Nature

Reserve, Zhangzhou City, Fujian Province (23°55'N, 117°26'E). Hypocotyls with similar size and maturity that had no mechanical damage or wormholes were selected and planted in clean river sand in 45 cm × 35 cm × 25 cm plastic trays. Twenty plants were planted in each tray and irrigated with 1 L of Hoagland nutrient solution. The diminished water was supplemented with distilled water every evening, and the nutrient solution was replaced every three days. The seedlings were treated with Hoagland nutrient solution containing different concentrations of NaCl (0, 200, 400, and 600 mmol L⁻¹ NaCl) after having grown to four leaves (60 days), labeled as the 0 mM, 200 mM, 400 mM, and 600 mM groups, respectively. Three plastic trays (namely three biological replicates) with each tray containing 20 seedlings were used in each NaCl treatment. After three days of treatment, all the roots in each treatment were cut off, quickly frozen in liquid nitrogen, and then stored at -80 °C to preserve them for future study.

2.2. Total RNA extraction and library construction

Total RNA was extracted from the roots of *K. candel* by the cetyltrimethylammonium bromide (CTAB)-LiCl precipitation method (Jordon et al., 2015). The qualified RNA with the required concentration, purity, integrity, and fragment size was used to construct the library according to the manufacturer's instructions (Yang et al., 2011). Briefly, RNA was incubated and broken in fragment buffer (Ambion, Austin, TX, USA). Subsequently, the first strand of DNA was synthesized using random hexamer primers (Illumina, San Diego, CA, USA) and reverse transcriptase (Invitrogen, Carlsbad, CA, USA); the second strand of DNA was synthesized by DNA polymerase I (Invitrogen, Grand, NY, USA), and the double strand of DNA fragments was purified by a QIAquick PCR extraction kit and connected to an Illumina transcription adapter (Yang et al., 2011). The suitable fragments were then selected for PCR amplification.

2.3. Illumina sequencing, assembly, and annotation analysis

After the quality test of the constructed library was qualified, transcriptomic sequencing was performed using an Illumina HiSeq 2000 platform according to the manufacturer's instructions. The original reads (double-ended sequences) were evaluated, and the raw 100 bp paired-end reads were generated. The clean reads were obtained by removing low-quality reads containing more than 20% unknown bases with a Q-value ≤10 and reads containing more than 5% unknown sequences "[N]". Simultaneously, the quality parameters of the clean read data including Q30 (percentage of bases with a Phred value >30) and GC-content were calculated. Subsequently, de novo transcriptome assembly of these clean reads was performed by using Trinity software (v2012-10-05)

with `min_kmer_cov` set to 2 and other default settings (Grabherr et al., 2011). The main transcript more than 200 bp of genes was selected as the unigene. The assembled *K. candel* unigenes were BLASTed against NCBI Nonredundant protein (Nr)¹ (Deng et al., 2006), Kyoto Encyclopedia of Genes and Genomes (KEGG)² (Kanehisa et al., 2008), Clusters of Orthologous Groups (COG)³ (Tatusov et al., 2000), Gene Ontology (GO)⁴ (Ye et al., 2006), and Swiss-Prot⁵ (Apweiler et al., 2004) to obtain the functional annotations.

2.4. Analysis of differentially expressed genes (DEGs)

RSEM software was used for a bowtie comparison between the sequencing reads of each sample and the Unigene sequence with nucleotide mismatches with the set of no more than 2 by default (Trapnell et al., 2009). The results of RSEM alignment were counted to obtain the number of reads on the corresponding Unigene sequence for each sample alignment. Then, the gene expression level for each Unigene was further estimated accordingly by using reads per kilobase per million (RPKM) with the RPKM value as each gene expression (Mortazavi et al., 2008).

The DEGs in the 200/0 mM, 400/0 mM, and 600/0 mM groups were defined according to the screening criteria of a fold change ratio set to more than 2 (namely RPKM 200 mM/RPKM 0 mM ≥ 2 , RPKM 400 mM/RPKM 0 mM ≥ 2 , and RPKM 600 mM/RPKM 0 mM ≥ 2) and a false discovery rate (FDR) ≤ 0.01 . To evaluate the biological function of the DEGs, GO and KEGG analyses in the 200/0 mM, 400/0 mM, and 600/0 mM groups were performed, respectively. A hierarchical cluster analysis of the DEGs was performed by using Cluster 3.0 software.

2.5. Quantitative real time-PCR (qRT-PCR) analysis of DEGs

Total RNA from the *K. candel* roots was also extracted using the CTAB-LiCl precipitation method (Jordon et al., 2015). Twelve DEGs were selected and analyzed by qRT-PCR using the housekeeping gene *Actin* as the internal reference gene (Wang et al., 2016). The primers which were designed according to the sequences obtained from transcriptome sequencing data were listed in Table 1 (see also Table S1). qRT-PCR analysis was performed on a Bio-Rad CFX Connect™ real-time PCR system (Hercules, CA, USA) by using a SYBR Premix Ex Taq™ kit (TaKaRa, Tokyo, Japan) according to the manufacturer's instructions. The expression level of each gene was calculated by using the $2^{-\Delta\Delta Ct}$ method (Livak and Schmittgen, 2001). Three biological replicates were used for each DEG.

2.6. Detection of physiological and biochemical parameters

2.6.1. Determination of antioxidant system-related enzyme activities and substance contents

The methods of hydroxylamine oxidation (Wang and Luo, 1990), titanium-hydroperoxide complex (Patterson et al., 1984a) and thiobarbituric acid (Saradhi and Mohanty, 1993) were used to determine the contents of superoxide anion ($O_2^{\cdot-}$), hydrogen peroxide (H_2O_2), and malondialdehyde (MDA), respectively. The activities of superoxide dismutase (SOD) and peroxidase (POD) were measured using the nitroblue tetrazole photoreduction (Hyland et al., 1983) and guaiacol (Yu et al., 2011) methods, respectively. The assays of catalase (CAT), ascorbic acid peroxidase (APX), and glutathione reductase (GR) activities were conducted according to the methods as described by Patterson et al. (1984b), Nakano and Asada (1981), and Halliwell and Foyer (1978), respectively. The ascorbic acid (AsA) and reduced glutathione (GSH) contents were determined as previously described by Law et al. (1983) and Guri (1983), respectively.

2.6.2. Determination of respiration-related enzyme activities and metabolites

The activities of pyruvate kinase (PK) and pyruvate decarboxylase (PDC) and the pyruvate content were determined according to the manufacturer's instructions of commercial kits (Nanjing Jiancheng Bioengineering Institute, Nanjing, China).

The activities of fructose 6-phosphate kinase (PFK), malate dehydrogenase (MDH), isocitrate dehydrogenase (IDH), succinate dehydrogenase (SDH) and the content of ATP were determined according to the manufacturer's instructions of their corresponding kits (Suzhou Keming Biotechnology Co., Ltd., China).

2.6.3. Determination of osmoregulatory substances

The content of free proline (Pro) was determined by the sulfosalicylic acid method (Bates et al., 1973), and the content of glutamate (Glu) was determined by using a commercial kit (Suzhou Keming Biotechnology Co., Ltd., Suzhou, China). The gamma amino butyric acid (GABA) content was determined by a GABA ELISA kit (Nanjing Jiancheng Bioengineering Institute, Nanjing, China).

For each experiment on the physiological and biochemical parameters above, at least three independent biological replicates were performed. The results were shown as the mean \pm standard deviation (SD). A statistical analysis was performed using an analysis of variance

¹ <http://www.ncbi.nlm.nih.gov>

² <http://www.genome.jp/kegg>

³ <http://www.ncbi.nlm.nih.gov/COG>

⁴ <http://wego.genomics.org.cn/>

⁵ <https://www.ebi.ac.uk/uniprot/>

Table 1. Primer pairs used for quantitative real-time PCR.

NO.	Primer	Gene ID	Gene function	Primer sequence (5'-3')
	<i>Actin-S</i>		Reference gene	AGCATCAGGCATCCATGAGAC
	<i>Actin-A</i>			TGCTGAGAGATGCCAGAATG
1	<i>STPK-S</i>	comp14622_c0	Serine/threonine-protein kinase	CCAGATGTGGGTGCCTCAAT
	<i>STPK -A</i>			TGTCGGACCAGACCTTTATGT
2	<i>ACS-S</i>	comp13811_c0	1-aminocyclopropane-1-carboxylate synthase	CAGTGGAAGTTGCTTTGGC
	<i>ACS -A</i>			GGGTGATTGAGGGATAGGAG
3	<i>TAT-S</i>	comp21802_c0	Tyrosine aminotransferase	AACAAAGACGACGATAGCAGG
	<i>TAT -A</i>			TGGGACATCACCGTAGGAGG
4	<i>ASO-S</i>	comp12835_c0	L-ascorbate oxidase	CGGTTATCGTCGTTGGTCT
	<i>ASO -A</i>			TCTCGCTATCGTTAGGTTTCA
5	<i>GST3-S</i>	ccomp13222_c0	Glutathione transferase 3	CCCAAAGACCCTTACAACAGA
	<i>GST3-A</i>			GAAACCAGTAGGCTATGGACAA
6	<i>TPS-S</i>	comp17959_c0	trehalose-6-phosphate synthase	GATTTTGCTTACCGCACTTG
	<i>TPS -A</i>			CTTATCTCGGCTTCTTCCACT
7	<i>AMT-S</i>	comp38647_c0	ammonium transporter	ATCTTGCTTGCTGGTTCTGTT
	<i>AMT -A</i>			CTATCGCTCTTTAGCCTTGGT
8	<i>Ca-ATPase-S</i>	comp7186_c0	Calcium ATPase 2 isoform 3	GCTTGTGCTCTGAAATCCC
	<i>Ca-ATPase -A</i>			GTTTATTATTTCCATTTTCCCTCCTCGA
9	<i>CaM-S</i>	comp11533_c0	Calmodulin	AAGGCATTTCGTGTTTCGTGA
	<i>CaM -A</i>			CATCATTTAGTGCTGGAGGG
10	<i>POD-S</i>	comp19686_c0	Peroxidase	CAAGCCTTTTCAAGCGTA
	<i>POD -A</i>			CGATTTTACTGGATTCTACCC
11	<i>SAMS2-S</i>	comp11749_c0	S-adenosylmethionine synthase 2	ACTTGAATCCGCTCTGGTCG
	<i>SAMS2-A</i>			TGGCAGCCTGTCTAACTATGT
12	<i>AP2/ERF-S</i>	comp23858_c0	AP2/ERF domain-containing transcription factor	CCAGCATTAGGCACCTTCA
	<i>AP2/ERF -A</i>			ATGGGATGTTTGCGGATTT

(ANOVA) and least significant difference (LSD) test to determine significant differences among the four groups. Statistical significance was considered at $P < 0.05$.

3. Results

3.1. Characteristics of transcriptomic sequencing assembly in the *K. candell* roots

In RNA-Seq, the transcript size, GC content, and sequencing depth are closely related to quality control. After quality control, a total of 65.79 M clean reads were obtained from eight samples of *K. candell* roots by transcriptomic sequencing, and the clean reads of each sample were more than 7.50 M. The total base number of each sample was 6.64 Gb, and the total base number of each sample was higher than 760 Mb. The base Q30 of each sample was higher than 86%, and the GC content of each sample was approximately 45% (Table 2). This result

showed that the quality of transcriptomic sequencing in the *K. candell* roots was relatively high.

Using a Trinity assembly platform, 112,243 transcripts and 61,970 unigenes were obtained, and the N50 of the transcripts and unigenes were 2361 bp and 1510 bp, respectively (Table 3). This result indicated that the assembly integrity of the root transcript fragments was relatively high in *K. candell*.

3.2. Statistics of DEGs in the *K. candell* roots under salt stress

According to $FDR < 0.01$ and a fold change ratio of more than 2 ($|\log_2 \text{Ratio}| \geq 1$) as screening criteria, a statistical analysis was performed on the DEGs among different treatments in Table 4. Compared with the 0 mM group, there were 454 DEGs (246 upregulated genes and 208 downregulated genes) under the 200 mM group, 311 DEGs (187 upregulated genes and 124 downregulated

Table 2. Sequencing assessment statistics of *K. candel* roots.

Sample	Total clean reads	Total cleannucleotides (nt)	GC (%)	Q30 (%)
0 mM-1	7,715,855	779,166,127	44.97%	86.83%
0 mM-2	7,881,189	795,881,180	45.01%	86.96%
200 mM-1	7,785,511	786,217,908	45.00%	86.78%
200 mM-2	7,735,691	781,185,251	45.08%	86.70%
400 mM-1	7,560,418	763,482,184	45.22%	86.86%
400 mM-2	9,548,303	964,240,229	45.31%	86.10%
600 mM-1	9,844,492	994,138,353	45.48%	86.13%
600 mM-2	7,715,855	779,166,127	44.97%	86.83%

Table 3. Summary of assembly quality of *K. candel* roots.

	Contigs	Transcripts	Unigenes
Total number	1,519,826	112,243	61,970
Total length	124,248,865	155,515,125	49,003,086
Mean length	81.75	1,385.52	790.75
N50 length	124	2361	1510

Table 4. The statistics of DEGs (DEGs) amount among different groups.

Groups	All DEGs	Upregulated DEGs	Downregulated DEGs
200/0 mM	454	246	208
400/0 mM	311	187	124
600/0 mM	2663	1701	962

genes) under the 400 mM group, and 2663 DEGs (1701 upregulated genes and 962 downregulated genes) under the 600 mM group. These results showed that the numbers of DEGs under the 200 mM NaCl and 400 mM NaCl treatments were significantly less than those under the 600 mM group, suggesting that the high salinity environment (600 mmol L⁻¹ NaCl) had a greater impact on gene expression in the *K. candel* roots.

A Venn diagram was used to count the DEGs screened (Figure S1). The results showed that there were 63 DEGs under three concentrations of NaCl treatments compared with the 0 mM group. Moreover, there were 184, 39, and 2212 DEGs under the 200 mM, 400 mM, or 600 mM groups, including 74, 36, and 1414 DEGs that were upregulated, respectively, and 157, 6, and 832 DEGs that were downregulated, respectively.

A hierarchical cluster was performed on the expression levels of DEGs in two biological replicates under four groups (Figure S2). The results showed that the expression patterns in each treatment were similar between the two biological replicates, but they were different among the four groups. The expression patterns between the 200 mM and 0 mM groups were slightly different, while those between the 600 mM and 0 mM groups were quite different.

3.3. GO classification and KEGG enrichment analysis of DEGs in the roots of *K. candel* under salt stress

The enriched GO function of the DEGs was classified and analyzed based on their cell components, molecular functions, and biological processes. The results are shown in Figure 1. In the 200/0 mM group, the DEGs were divided into 45 GO items. Among them, 13 GO items were identified as cell components, 11 GO items performed molecular functions, and 21 GO items participated in biological processes (Figure 1A). In the 400/0 mM group, the DEGs were divided into 44 GO items. Among them, 14 GO items were identified as cell components, 11 GO items performed molecular functions, and 19 GO items participated in biological processes (Figure 1B). In the 600/0 mM group, the DEGs were divided into 51 GO items. Among them, 14 GO items were identified as cell components, 13 GO items performed molecular functions, and 24 GO items participated in biological processes (Figure 1C).

Among the three groups, the cell part, cell, and organelle accounted for the largest proportion of cell components; catalytic activity and binding accounted for the largest proportion of molecular functions, and the cell processing, metabolic process, and stimulus response accounted for the highest proportion in biological processes.

The KEGG pathway enrichment analysis of DEGs ($P < 0.05$) was performed, and the results are shown in Table 5. In the 200/0 mM group, five pathways were

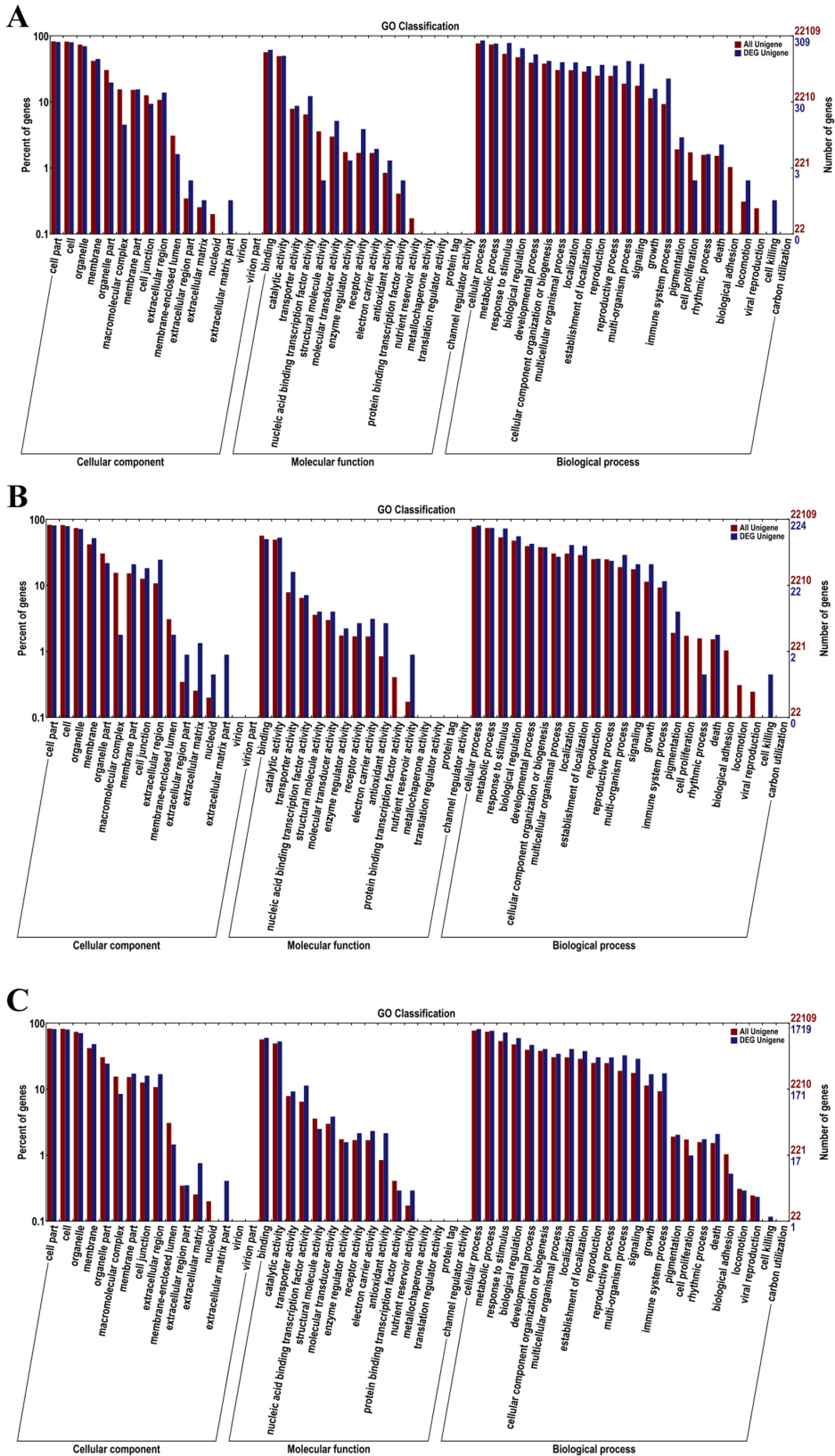


Figure 1. Gene ontology classification enrichment analysis of differentially expressed genes from *K. candell* roots under salt stress. A: 200/0 mM group; B: 400/0 mM group; C: 600/0 mM group.

Table 5. Enriched significant pathways related to DEGs in *K. candel* roots under salt stress.

KEGG_pathway	KO_ID	Cluter_frequency	P-value
200/0 mM			
Plant hormone signal transduction	ko04075	22.50%	0.0002
Cysteine and methionine metabolism	ko00270	15.00%	0.0012
Plant-pathogen interaction	ko04626	12.50%	0.0094
Brassinosteroid biosynthesis	ko00905	2.50%	0.0367
Sulfur metabolism	ko00920	5.00%	0.0413
400/0 mM			
Phenylpropanoid biosynthesis	ko00940	22.22%	0.0000
Phenylalanine metabolism	ko00360	18.52%	0.0001
Tropane, piperidine and pyridine alkaloid biosynthesis	ko00960	7.41%	0.0038
Glycerolipid metabolism	ko00561	11.11%	0.0054
Limonene and pinene degradation	ko00903	7.41%	0.0067
Pentose and glucuronate interconversions	ko00040	11.11%	0.0077
Lysine degradation	ko00310	7.41%	0.0088
Histidine metabolism	ko00340	7.41%	0.0130
Pyruvate metabolism	ko00620	11.11%	0.0208
Tryptophan metabolism	ko00380	7.41%	0.0220
Propanoate metabolism	ko00640	7.41%	0.0331
beta-Alanine metabolism	ko00410	7.41%	0.0358
Fatty acid metabolism	ko00071	7.41%	0.0414
Ascorbate and aldarate metabolism	ko00053	7.41%	0.0429
Flavone and flavonol biosynthesis	ko00944	3.70%	0.0431
Plant hormone signal transduction	ko04075	14.81%	0.0489
600/0 mM			
Phenylpropanoid biosynthesis	ko00940	1.64%	0.0000
Phenylalanine metabolism	ko00360	10.34%	0.0000
Plant-pathogen interaction	ko04626	11.21%	0.0000
Plant hormone signal transduction	ko04075	10.78%	0.0003
Tropane, piperidine and pyridine alkaloid biosynthesis	ko00960	1.72%	0.0070
Pentose and glucuronate interconversions	ko00040	3.88%	0.0082
Propanoate metabolism	ko00640	3.02%	0.0107
Biosynthesis of unsaturated fatty acids	ko01040	2.59%	0.0131
Glycolysis / Gluconeogenesis	ko00010	6.47%	0.0168
Glycosphingolipid biosynthesis - globo series	ko00603	1.29%	0.0185
Cysteine and methionine metabolism	ko00270	5.60%	0.0231
Isoquinoline alkaloid biosynthesis	ko00950	1.29%	0.0237
Flavonoid biosynthesis	ko00941	2.16%	0.0266
Pentose phosphate pathway	ko00030	3.45%	0.0383
Ubiquinone and other terpenoid-quinone biosynthesis	ko00130	2.16%	0.0464

enriched, and plant hormone signal transduction was the pathway with the most DEGs, followed by cysteine and methionine metabolism, plant-pathogen interaction, sulfur metabolism, and brassinosteroid metabolism. In the 400/0 mM group, 16 pathways were enriched, and phenylpropane metabolism was the pathway with the most DEGs, followed by phenylalanine metabolism, plant hormone signal transduction, and pyruvate metabolism. In the 600/0 mM group, 15 metabolic pathways were enriched, and phenylpropane biosynthesis was the pathway with the most DEGs, followed by phenylalanine metabolism, plant-pathogen interaction, plant hormone signal transduction, glycolysis and gluconeogenesis, cysteine methionine metabolism, and the pentose phosphate pathway.

Based on the results of the GO and KEGG pathway analyses, the candidate DEGs in the roots of *K. candell* under salt stress were primarily classified into plant hormone signal transduction, carbohydrate and energy metabolism, amino acid metabolism, and stress response and defense (Table 6).

3.4. qRT-PCR analysis of DEGs in the roots of *K. candell* under salt stress

Twelve DEGs involved in energy formation, signal transduction, stress response and defense were selected for qRT-PCR analysis (Figure 2). The results showed that the expression trend of these 12 DEGs was consistent with the results of RNA-Seq, indicating that the results of RNA-Seq were reliable.

3.5. Physiological characteristics of *K. candell* roots in response to salt stress

With the increase of NaCl concentration, the O_2^- and H_2O_2 content in the roots of *K. candell* increased to varying degrees, while those under the 600 mM group were significantly higher than those under the 0 mM group (Figure 3). This result indicated that the ROS increased and accumulated in the roots of *K. candell* under a high concentration of NaCl. However, the MDA content increased slightly under salt stress, but there was no significant difference among the four groups except high salt stress (600 mM NaCl), indicating that the membrane lipids of the root cells of *K. candell* were not seriously damaged by peroxidation under moderate salt stress (400 mM NaCl).

The activities of antioxidant enzymes and the content of antioxidant substances in the roots of *K. candell* were determined under different concentrations of NaCl. The results showed that the activities of SOD, POD, CAT, APX, and GR increased significantly under different concentrations of NaCl compared with the 0 mM group. Simultaneously, the contents of antioxidants, including GSH and AsA, increased significantly with the increase in NaCl concentration. These results indicated that the *K. candell* roots could improve the antioxidant system and maintain the dynamic balance of ROS under salt stress.

EMP-TCA is the primary source of plant energy. The transcriptomic analysis showed that the genes related to the EMP-TCA pathway were upregulated in the *K. candell* roots under salt stress. Therefore, the key enzymes and their metabolites in EMP-TCA pathway were determined in this study. The results are shown in Figure 4. Compared with the 0 mM group, the activities of PFK, PK, PDC, IDH, SDH, and MDH in EMP-TCA increased significantly in the 600 mM group, and the trend of the change in the pyruvate content and the levels of energy ATP were consistent with those of the enzyme activities. These results indicated that the *K. candell* roots could maintain the normal progress of EMP-TCA and provide sufficient energy for the plants to perform various types of biochemical metabolism to completely resist salt stress.

Under salt stress, the contents of Glu and GABA in the roots of *K. candell* accumulated with the increase in the concentration of NaCl. However, the contents of Pro did not change significantly under different concentrations of NaCl (Figure 5). This result indicated that the *K. candell* roots could enhance salt tolerance by accumulating osmotic regulators, such as Glu and GABA.

4. Discussion

4.1. Genes related to ethylene and protein kinase signal transduction

Plant hormone signal transduction plays an important role in plant responses to environmental stresses (Colebrook et al., 2014). In plants, ethylene is synthesized by the Yang Cycle. Briefly, methionine (Met) is catalyzed by SAMS to produce SAM; SAM produces ACC and 5'-methylthioadenosine under the action of ACS, and the ACC generated produces ethylene under the catalysis of ACO (Bleecker and Kende, 2000). ACS is the key enzyme and rate-limiting enzyme for ethylene synthesis in plants, and the ACS activity determines the production of ethylene. Previous studies have found that high salt stress could induce the expression of ACS5 and ACS7 genes in *Arabidopsis thaliana* (Wang et al., 2005) and also upregulate the expression of *NtACS1* gene in tobacco (Cao et al., 2006). Therefore, salt stress can promote ethylene synthesis in plants and improve salt tolerance (Achard et al., 2006). In this study, the results of RNA-Seq and qRT-PCR both indicated that the *SAMS2*, *ACS*, *ACO*, and *ERF114* genes which related to ethylene synthesis were significantly upregulated in the roots of *K. candell* under salt stress. Meanwhile, the antioxidant enzyme activities and antioxidant contents were also remarkably increased (Figure 3). These results suggested that the increase of ethylene synthesis might stimulate the activity of intracellular ROS scavenging system by increasing the enzyme activities and antioxidant contents to enhance salt tolerance in *K. candell* roots under salt stress.

Table 6. Key candidate genes responding to salt stresses in *K. candel* roots.

Transcript ID	Description	Gene name	log ₂ (RPKM)		
			200/0 mM	400/0 mM	600/0 mM
Carbohydrate and energy metabolism					
comp20102_c0	Fructose-1,6-bisphosphate aldolase	<i>FBA</i>	0.7300	0.8600	1.1625
comp15041_c0	6-phosphofructokinase 3	<i>PFK3</i>	0.4256	0.3020	1.2798
comp28319_c0	Malate dehydrogenase	<i>MDH</i>	0.5857	0.8743	2.5402
comp19852_c0	Aldehyde dehydrogenase	<i>ALDH</i>	-0.1058	0.7869	1.2688
comp11304_c0	UDP-glucuronate 4-epimerase	<i>GAE</i>	-0.4870	1.1096	1.2407
comp10686_c0	Plasma membrane ATPase	<i>ATPase</i>	0.4065	1.1405	1.3357
comp28922_c0	Cytochrome c oxidase	<i>COX</i>	0.5843	1.3487	2.8396
comp5865_c0	Fructose-bisphosphate aldolase	<i>FBA</i>	0.8982	0.7667	1.6589
comp15041_c0	6-phosphofructokinase	<i>PFK</i>	0.2812	0.6084	1.3444
comp17096_c0	6-phosphogluconate dehydrogenase	<i>6PGDH</i>	0.3727	0.6271	1.4829
comp16296_c0	Glucose-6-phosphate 1-epimerase	<i>GPE</i>	0.5828	1.7152	2.1555
comp18495_c0	Phosphoglycerate kinase	<i>PGK</i>	0.8942	1.0283	1.0422
comp19497_c0	Pyruvate kinase	<i>PK</i>	0.4771	0.9434	1.0565
comp22494_c0	Fructokinase	<i>FK</i>	0.5409	0.4244	1.1327
comp19264_c0	ATPase E1-E2 type familyATPase	<i>ALA9</i>	0.1936	0.3674	1.2032
comp19507_c1	Aconitate hydratase 2	<i>ACO2</i>	0.5212	0.5526	1.0335
comp20175_c0	NADP-dependent malic enzyme	<i>Me1</i>	-0.4622	0.8306	1.4255
comp20273_c0	Citrate synthase	<i>CS</i>	0.6162	0.9000	1.3140
comp11233_c0	Succinate dehydrogenase	<i>SDH1</i>	0.9553	1.0923	1.1576
Amino acid metabolism					
comp23536_c0	Glutamate synthase	<i>GS</i>	1.2033	0.6936	1.4030
comp18579_c1	Glutamate dehydrogenase	<i>GDH</i>	0.5784	0.7095	1.2895
comp16757_c0	Glutamate decarboxylase	<i>GAD</i>	-0.3030	0.7355	1.5542
comp15922_c0	Cysteine synthase	<i>CyS</i>	1.2047	0.9473	2.3068
comp69612_c0	Pyrroline-5-carboxylate synthetase	<i>P5CS</i>	0.7345	1.1902	1.3300
comp24593_c0	Proline dehydrogenase 2	<i>PDH2</i>	0.5044	1.1391	1.7871
comp11445_c0	Spermine synthase	<i>SPDS</i>	0.6318	0.8121	1.7412
comp27633_c0	Thermospermine synthase	<i>ALC5</i>	-0.7790	0.5322	1.1804
comp22406_c0	Cysteine desulfurase 1	<i>CyD1</i>	0.5270	0.4739	1.1244
comp24982_c0	S-adenosylmethionine-dependent methyltransferase	<i>SDMF</i>	-0.8975	0.7775	3.0489
comp10465_c0	S-adenosylmethionine decarboxylase	<i>SAMD</i>	0.3657	0.2016	1.4018
Plant hormone signal transduction					
comp11749_c0	S-adenosylmethioninesynthetase 2	<i>SAMS2</i>	0.3564	0.6783	1.9134
comp13811_c0	1-aminocyclopropane-1-carboxylate synthase	<i>ACS</i>	-	2.0893	4.2977
comp20158_c0	1-aminocyclopropane-1-carboxylate oxidase	<i>ACO</i>	0.6990	0.5754	1.4193
comp16642_c0	Ethylene receptor 2	<i>ETR2</i>	-	-1.8900	-1.0600
comp79252_c0	Ethylene receptor 1	<i>ETR1</i>	-0.8900	-1.1934	1.8700
comp25493_c0	Protein EIN4	<i>EIN4</i>	-	-1.0300	-1.5700
comp15173_c0	Ethylene-responsive transcription factor ERF114	<i>ERF114</i>	-0.6141	2.3159	4.0551
comp10075_c1	Mitogen-activated protein kinase 3	<i>MAPK3</i>	0.3688	0.1545	1.2508

Table 6. (Continued).

comp15128_c0	Mitogen-activated protein kinase kinasekinase	MAPKKK	0.6179	-0.7185	1.4595
comp18149_c0	Calcium-dependent protein kinase 10	CDPK10	0.5658	0.6889	1.1117
Stress response and defense					
comp13222_c0	Glutathione transferase 3	GST3	0.5864	1.0516	1.2149
comp20820_c0	Thioredoxin reductase 2	TRXR	0.5712	0.4537	1.0842
comp19680_c0	Cationic peroxidase 1	POD1	4.3802	5.1077	7.1232
comp13288_c0	Fe-superoxide dismutase	Fe-SOD	1.0234	1.7595	1.7641
comp19754_c1	Superoxide dismutase [Mn]	Mn-SOD	0.3057	0.5606	1.0309
comp144320_c0	Superoxide dismutase [Cu-Zn]	Cu/Zn-SOD	-0.6978	0.5662	1.0583
comp9884_c0	Glutathione peroxidase 2	GPX2	0.8655	1.6669	1.9636
comp1005_c0	Catalase-3	CAT3	-	-	3.0975
comp6225_c0	Glutathione reductase	GR	-0.2273	1.2946	3.1185
comp10159_c0	Glutaredoxin-C9	GRX	1.3251	0.3655	2.2602

The ethylene signaling pathway contains not only many ethylene receptors, such as ETR1, ETR2, ERS2, and EIN4, but also signal pathway inhibitors (CTR1 and EIN2), a related transcription factor (EIN3/EIL1) and downstream functional genes (Guo and Ecker, 2004). EIN2 positively regulates salt tolerance in *Arabidopsis thaliana* (Lei et al., 2011). This study revealed that the corresponding genes of ETR1, ETR2, and EIN4 in the *K. candel* roots were differentially expressed under salt stress, indicating that the ethylene signaling pathway was enhanced by *K. candel* under salt stress in the manner as that discovered in *Avicennia officinalis* (Krishnamurthy et al., 2017).

Protein kinases also play an important role in plant hormone signal transduction. A previous study reported that AtMEK1 is involved in signal transduction during drought, high salinity, and mechanical injury (Huang et al., 2000). *AtMCK2* is specifically activated by high salinity and AtMK1, and overexpression of the *AtMCK2* gene can enhance plant salt tolerance (Dubouzet et al., 2003). Currently, the salt stress-related MAPK pathway has been found in tobacco and alfalfa (Kiegerl et al., 2000). CDPK is a serine/threonine protein kinase that is found widely in plants, which can be activated under abiotic stress (Hwang et al., 2002). The overexpression of *OsCPK4* and *OsCDPK7* in rice can strongly enhance water-holding capability and reduce the levels of membrane lipid peroxidation and electrolyte leakage, thus improving salt tolerance under drought and high salt stress (Campo et al., 2014). In this study, we found that both the *MAPK* and *CDPK* genes were upregulated under high salt stress, indicating that these genes might be involved in the salt-stress responses in the *K. candel* roots.

4.2. Genes related to carbohydrate and energy metabolism

Plants need to resist salt stress by upregulating multiple biological processes, including the biosynthesis of osmotic

regulators, antioxidants, and antioxidant enzymes, all of which require energy consumption (Mittler 2002). Therefore, carbohydrate and energy metabolism are very important in plant salt tolerance. Under salt stress, most of the DEGs involved in the EMP-TCA pathway were upregulated, including the fructose-1,6-diphosphate aldolase (*FBA*), *PFK*, *PK*, citrate synthase (*CS*), *SDH* and *MDH* genes. Moreover, the activities of key enzymes in the EMP-TCA pathway, including *PFK*, *PK*, *MDH*, *IDH*, *SDH*, and *PDC*, significantly increased under high salt stress, indicating that aerobic respiration in the root was enhanced under salt stress. Oxidative phosphorylation is the most important source of energy for cells in the EMP-TCA metabolic pathway, and maintaining the efficient operation of the oxidative phosphorylation level is of substantial significance for plants to resist salt stress. In this study, eight DEGs, including two plasmalemma ATPase genes (*PMA4*), one *H⁺-pyrophosphatase* gene (*H⁺-PPase*), three *cytochrome C oxidase* genes (*COX3*, *COX6A*, and *COX17*), one *acyl carrier protein* gene (*ACP*), and one *NADP-quinone oxidoreductase* gene (*NDB3*), were significantly enriched and upregulated during oxidative phosphorylation in the roots of *K. candel* under salt stress. This indicated that the *K. candel* roots could upregulate the genes of respiratory electron transfer-related proteins and ATP synthase under salt stress, thus providing energy for the cells to resist salt stress.

In addition, aldehyde dehydrogenase (*ALDH*) can catalyze the oxidation of aldehydes to carboxylic acid; remove aldehydes, ketones, hydrocarbons and hydroxyl acids produced by membrane lipid peroxidation under salt stress; and improve plant salt tolerance (Jimenez, 2016). In this study, two *ALDH* genes were upregulated under salt stress, suggesting that *ALDH* might be involved in the removal of aldehydes and other harmful substances in the roots of *K. candel* under salt stress.

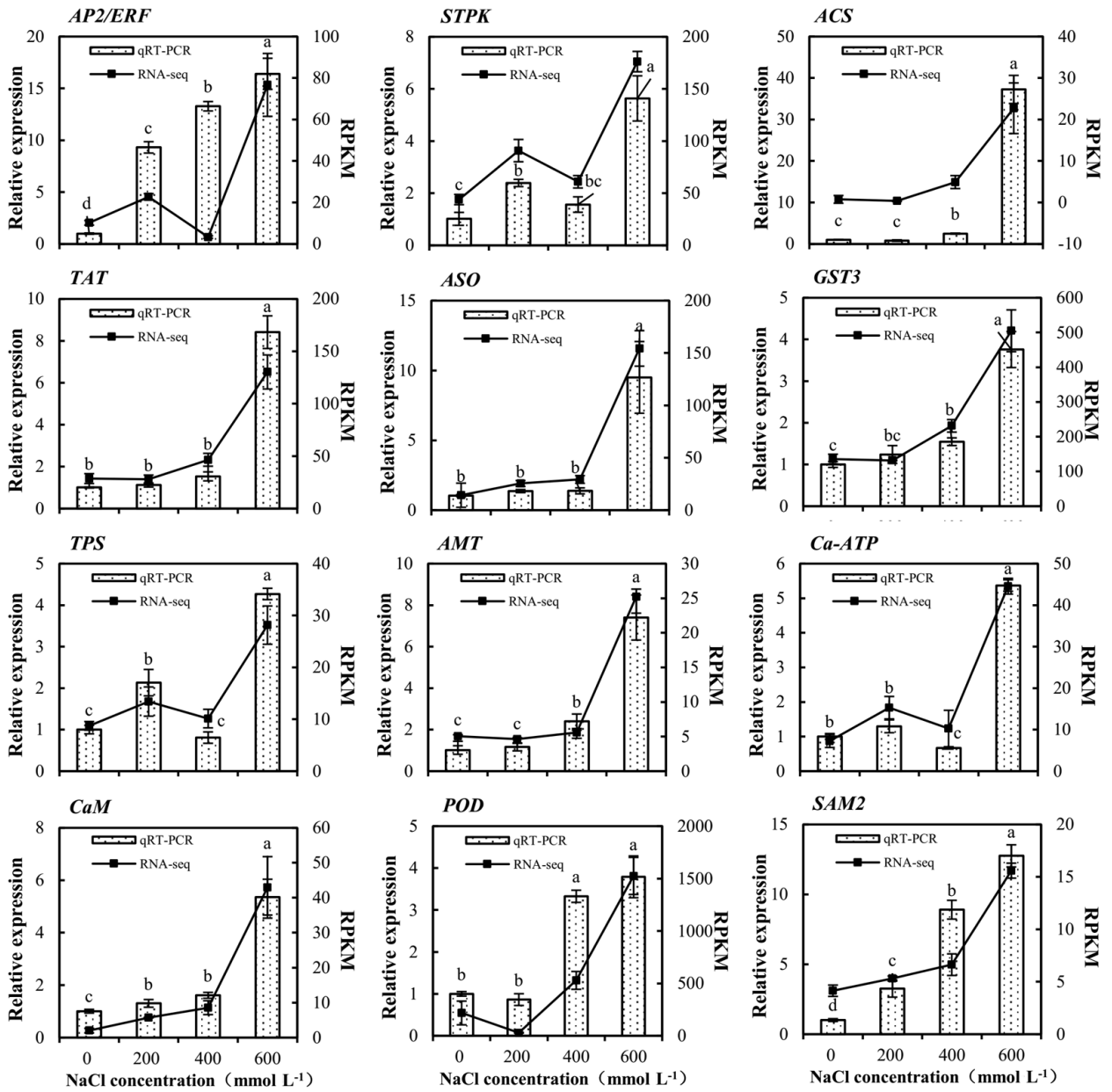


Figure 2. Quantitative RT-PCR analysis of differentially expressed genes in *K. candell* roots under salt stress. The values (black plots) are presented as mean \pm standard deviation for the fold changes in expression observed in the qRT-PCR analysis from three biological replicates for each salt concentration in the study. Different letters above the black plots indicate a significant difference at $P < 0.05$. The axes represent both the RPKM values obtained for each gene in the RNA-Seq analysis (gray bars).

4.3. Genes related to antioxidant system

When plants are exposed to salt stress, the cells accumulate a large amount of ROS, and such excesses will result in oxidative damage to DNA, proteins, lipids, and other biological macromolecules (Gill and Tuteja, 2010). Therefore, the participation of the antioxidant system is necessary to maintain the balance of ROS. The expression changes of some genes related to antioxidant system were found in this study. Gene expressions of *GST3*,

POD1, *Fe-SOD*, *GPX2*, and *GR* were upregulated under NaCl treatments with three different concentrations. In addition, gene expressions of *Mn-SOD*, *Cu/Zn-SOD*, *GRX*, and *CAT3* were not significantly changed under 200 and 400 mM NaCl treatments while they were upregulated under 600 mM salt stress, indicating that these genes were only induced under high salt stress in *K. candell* roots. Furthermore, the ROS and MDA content did not increase significantly except 600 mM salt treatment, suggesting that

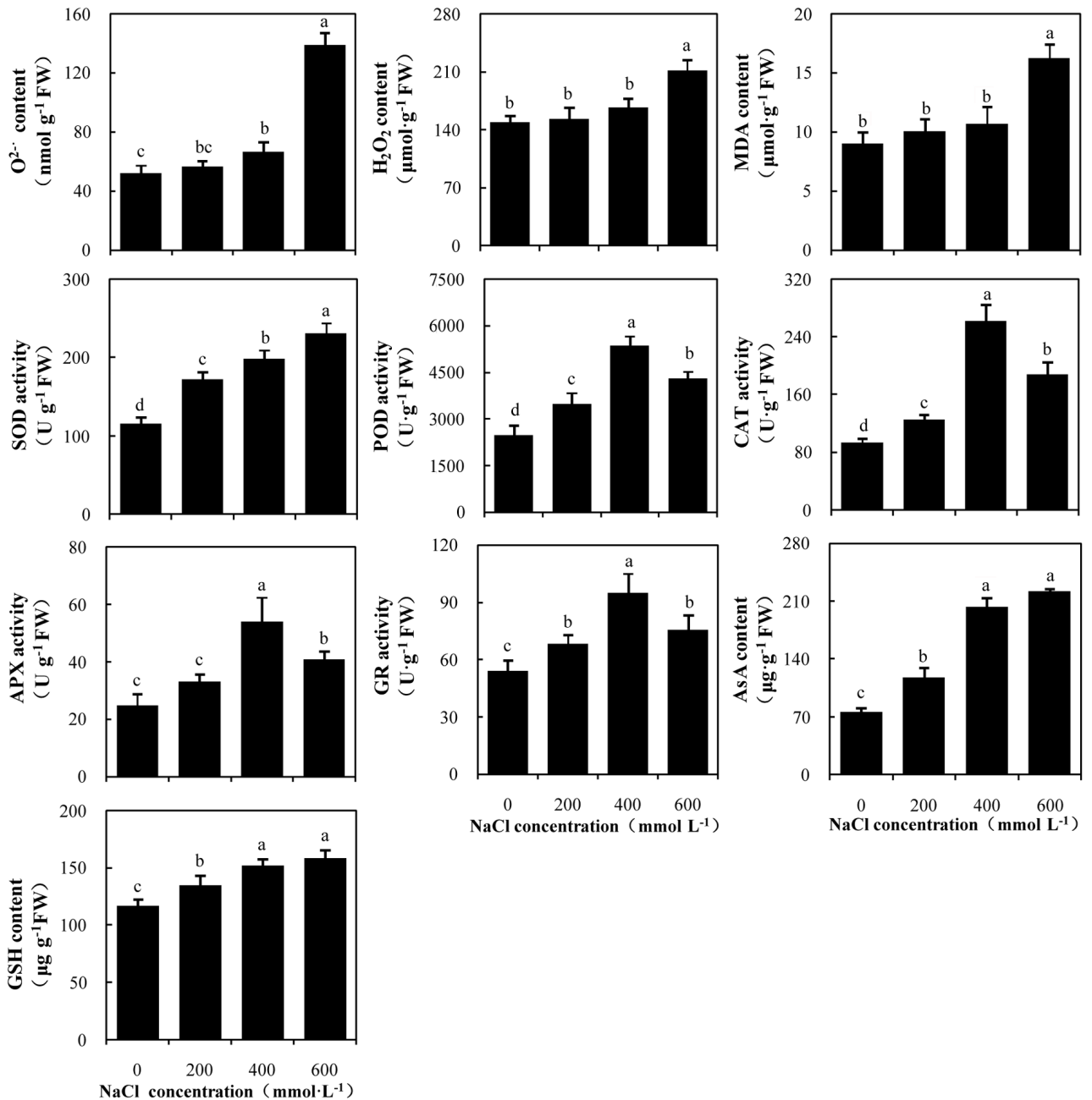


Figure 3. Changes of antioxidative ability in *K. candell* roots under salt stress. The values are presented as means \pm standard deviation for the changes of antioxidative ability from three biological replicates in the study. Different letters above the bars indicate a significant difference at $P < 0.05$.

K. candell could resist moderate salt stress. In antioxidant systems, SOD is a type of metalloenzyme that exists in plastids and can rapidly convert O₂^{·-} free radicals into H₂O₂, which is degraded by POD or CAT (Alscher et al., 2002). It has been found that the activities of POD and SOD in the leaves of *K. candell* increased significantly under salt stress (Wang et al., 2015). Our data showed that the activities of SOD, POD, and CAT in the roots of *K.*

candell were also significantly enhanced under salt stress. These results indicated that SOD, POD, and CAT could play an important role in scavenging ROS.

Moreover, the AsA-GSH circulatory system can also participate in scavenging the ROS in plants. In the AsA-GSH cycle system, AsA can reduce H₂O₂ to H₂O with the participation of APX, GPX, and other peroxidases, while AsA is oxidized to monodehydroascorbic acid

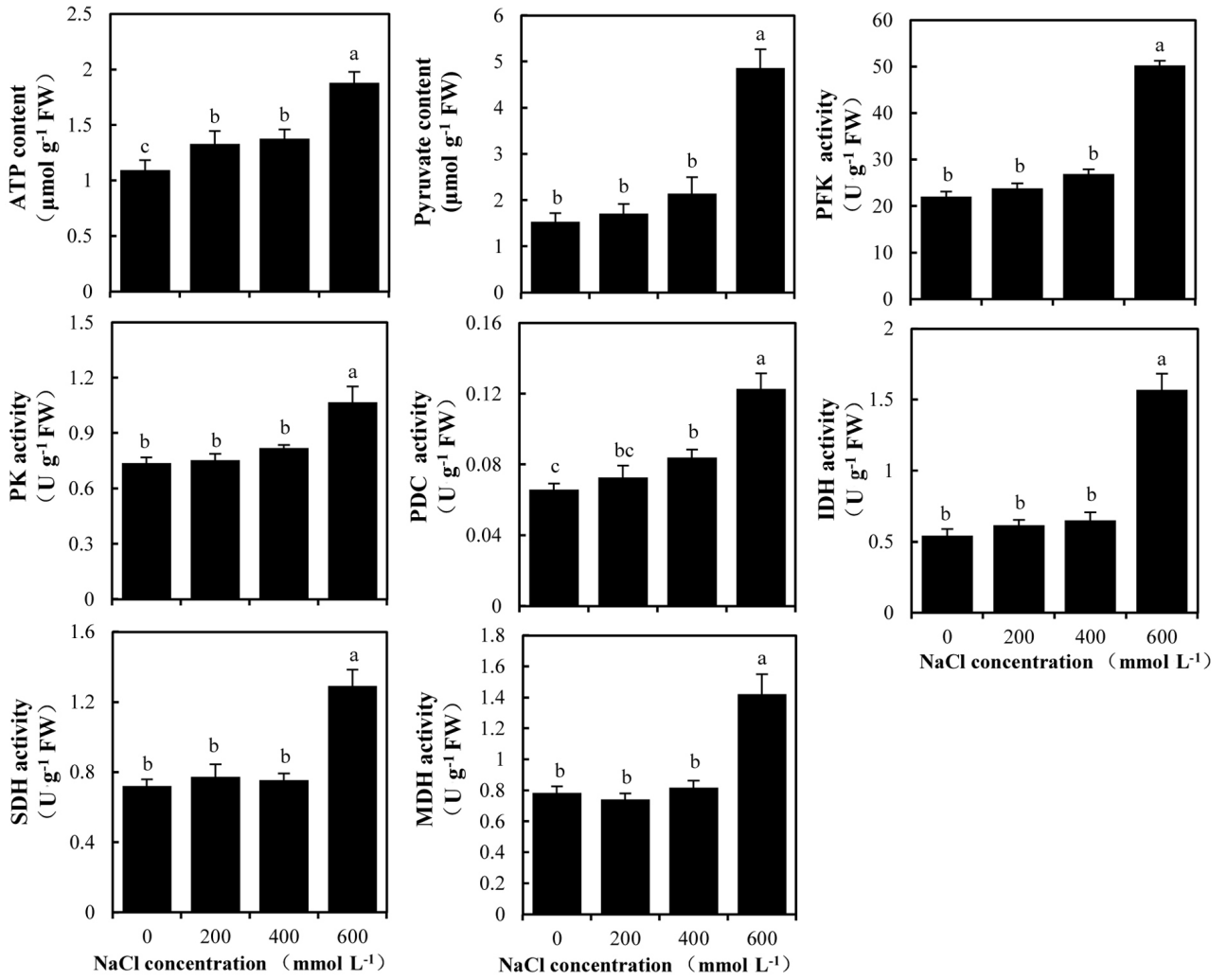


Figure 4. Changes of enzyme activity and product contents in the EMP-TCA pathway in *K. candel* roots under salt stress. The values are presented as means ± standard deviation for the changes of enzyme activity and product contents in the EMP-TCA pathway from three biological replicates in the study. Different letters above the bars indicate a significant difference at P < 0.05.

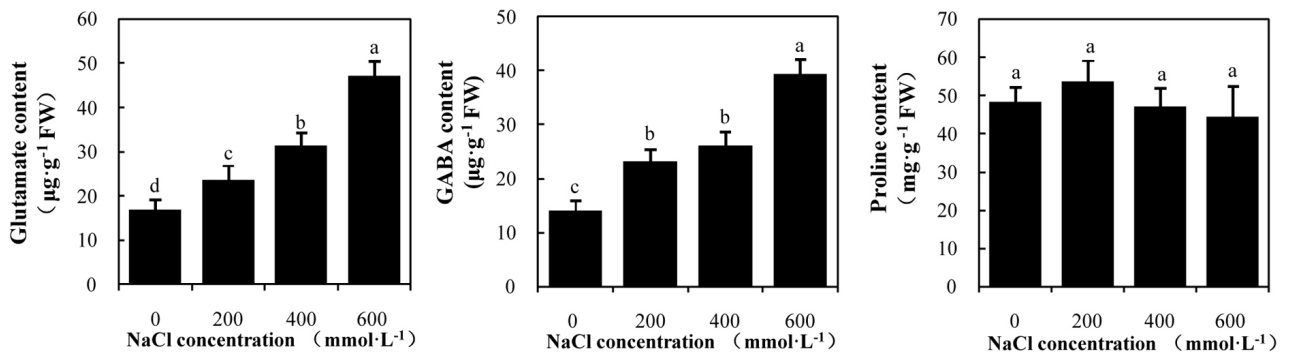


Figure 5. Changes in the contents of Glu, GABA, and Pro in *K. candel* roots under salt stress. The values are presented as means ± standard deviation for the changes of Glu, GABA, and Pro contents from three biological replicates in the study. Different letters above the bars indicate a significant difference at P < 0.05.

(MDHA) and dehydroascorbic acid (DHA). DHA can form AsA and produce oxidized glutathione (GSSG) with the participation of GSH. GSSG is catalyzed by GR to form GSH with the participation of NADPH. Moreover, under the action of glutathione transferase (GST), GSH can combine with peroxides and free radicals to scavenge ROS and protect the sulfhydryl groups of proteins in the cell membranes from being destroyed. Previous studies revealed that a high concentration of NaCl stress can promote the regeneration and biosynthesis of AsA in the roots and stems of *Jujube* to alleviate salt damage to *Jujube* seedlings (Lü et al., 2016). The GSH content and APX activity significantly increase in the leaves of *K. candel* under salt stress. This study also found that the contents of AsA and GSH, the activities of GR and APX, and the expression levels of related genes (*GST3* and *GPX2*) were significantly increased in the *K. candel* roots under salt stress. Our data showed that the genes involved in antioxidant defense systems were upregulated, the antioxidant enzyme activities were enhanced, and the antioxidant contents were increased in *K. candel* roots under salt stress. Furthermore, ROS and MDA contents were not increased obviously under moderate salt stress which due to the balance between ROS production and its scavenging capacity in *K. candel* roots. However, ROS and MDA contents increased significantly while ROS generating rate exceeded its scavenging rate, which might lead to lipid membrane damage by peroxidation under high salt stress.

In addition, thioredoxin (TRX) is a type of low molecular weight protein that is widely distributed in organisms and can regulate the intracellular redox potential (Kekulandara et al., 2018). NADPH, TRXs, and TRX reductase (TRXR) comprise the TRX system in plants and participate in intracellular redox reactions (Holmgren et al., 2009). Glutaredoxin (GRX) is GSH-dependent oxidoreductase, which forms the GRX system with GSH, NADPH, and GR in plants (Rouhier et al., 2002), and participates in the maintenance of the redox state and the regulation of redox-dependent signal pathway. Previous studies showed that the overexpression of the *SlGRX1* gene in tomato (Guo et al., 2010) or the *OsGRX6* gene in *Arabidopsis* (Sharma et al., 2013) can enhance the tolerance to environmental stresses, such as oxidation, high salinity, and osmosis. In this study, the *TRXR*, *GRX*, and *GSH* genes were upregulated in *K. candel* roots under salt stress, suggesting that both the TRX and GRX systems were involved in the salt-stress responses in *K. candel* roots. In conclusion, the antioxidant system plays an important role in the salt tolerance of the *K. candel* roots, which might respond to the oxidative damage caused by salt stress by coordinating various antioxidant enzymes and antioxidants.

4.4. Genes related to Glu and GABA biosynthesis

Amino acids are important nitrogen metabolites in plants and play an important role in plant resistance to stress (Szabados and Saviouré, 2010). Under salt stress, plants accumulate free amino acids as small organic molecules to participate in cell osmotic regulation, thereby avoiding salt-stress damage to plant cells (Munns, 2002). Glu is the center of amino acid metabolism in plants and the precursor of amino acid synthesis that produces compounds such as Pro and GABA (Forde and Lea, 2007). Glu can produce GABA by the catalysis of GAD or Pro by the catalysis of P5CS while Pro is oxidized to pyrroline-5-carboxylic acid by proline dehydrogenase (PDH). GABA and Pro can be used as osmotic regulators to regulate the balance of plant internal environment (Akçay et al., 2012). Wang et al. (2016) found that the contents of Glu and GABA in *K. candel* leaves increased significantly, but the contents of Pro did not change obviously under salt stress. In the present study, both *P5CS* and *PDH2* genes were upregulated, which could explain why Pro was not accumulated with salt treatments in *K. candel* roots. Under salt stress, Glu synthase (GS) and Glu dehydrogenase (GDH), two key enzymes in Glu metabolism in *K. candel* roots, were significantly upregulated at the transcriptional level. Obviously, the significant increase of the Glu content in the roots of *K. candel* under salt stress confirmed that the upregulation of the *GS* and *GDH* genes enhanced Glu biosynthesis, which was consistent with the results of Wang et al. (2016). Furthermore, the gene expression level of GAD, a key enzyme in GABA biosynthesis in the *K. candel* roots, was significantly upregulated, which enhanced GABA biosynthesis. Consistent with the findings described by Wang et al. (2016), we found that the salt stress induced the synthesis of Glu and GABA in the roots and enhanced the salt tolerance of *K. candel*.

Taken together, in this study, we provided a unique report on transcriptomic analyses of the nonsalt-secreting mangrove *K. candel* roots under salt stress. Our results suggested that the roots significantly enhanced the ethylene signal transduction pathway to regulate physiological metabolism, promoted aerobic respiration, and oxidative phosphorylation to maintain cell energy supply, increased the activities of various antioxidant enzymes and the antioxidant content to scavenge ROS. Notably, Glu and GABA were accumulated to improve cellular osmoregulatory ability and structural stability in *K. candel* roots, while the Pro content remained relatively stable under salt stress, which was not similar with the amino acid accumulation in glycophytes and nontree halophytes. These findings not only provide new insights into the molecular mechanisms of salt tolerance in mangroves, but also provide a new genetic resource for breeding transgenic salt-tolerant plants in the future.

Acknowledgements

This work was supported by the Chinese National Natural Science Funds (Grant no.331070542), the Natural Science Foundation of Fujian Province, China (Grant no. 2019J01819), Forestry Scientific Research Projects in Public Interest of China (Grant no. 201504415) and the

Higher School of Applied Discipline Construction Project of Fujian Province, China (No. 44 document in 2017). There was no additional external funding received for this study. The funders had no role in study design, data collection and analysis, decision to publish, or preparation of the manuscript.

References

- Achard P, Cheng H, De Grauwe L, Decat J, Schoutteten H et al. (2006). Integration of plant responses to environmentally activated phytohormonal signals. *Science* 311: 91-94. doi: 10.1126/science.1118642
- Akçay N, Bor M, Karabudak T, Ozdemir F, Türkan I (2012). Contribution of Gamma amino butyric acid (GABA) to salt stress responses of *Nicotiana sylvestris* CMSII mutant and wild type plants. *Journal of Plant Physiology* 169: 452-458. doi: 10.1016/j.jplph.2011.11.006
- Alscher R G, Erturk N, Heath L S (2002). Role of superoxide dismutases (SODs) in controlling oxidative stress in plants. *Journal of Experimental Botany* 53: 1331-1341. doi: 10.1093/jxb/53.372.1331
- Apweiler R, Bairoch A, Wu CH, Barker WC, Boeckmann B, Ferro S, Gasteiger E, Huang H, Lopez R, Magrane M (2004). UniProt: the universal protein knowledgebase. *Nucleic Acids Research* 32: D115-9. doi: 10.1093/nar/gkh131
- Bates LS, Waldren RP, Teare ID (1973). Rapid determination of free proline for water-stress studies. *Plant and Soil* 39: 205-207. doi: 10.1007/BF00018060
- Bleecker AB, Kende H (2000). Ethylene: a gaseous signal molecule in plants. *Annual Review of Cell and Developmental Biology* 16: 1-18. doi: 10.1146/annurev.cellbio.16.1.1
- Campo S, Baldrich P, Messegueur J, Lalanne E, Coca M et al. (2014). Overexpression of a calcium-dependent protein kinase confers salt and drought tolerance in rice by preventing membrane lipid peroxidation. *Plant Physiology* 165: 688-704. doi: 10.1104/pp.113.230268
- Cao WH, Liu J, Zhou QY, Cao YR, Zheng SF et al. (2006). Expression of tobacco ethylene receptor NTHK1 alters plant responses to salt stress. *Plant, Cell & Environment* 29: 1210-1219. doi: 10.1111/j.1365-3040.2006.01501.x
- Colebrook EH, Thomas SG, Phillips AL, Hedden P (2014). The role of gibberellin signalling in plant responses to abiotic stress. *Journal of Experimental Botany* 217: 67-75. doi: 10.1242/jeb.089938
- Cram J W, Torr P G, Rose D A (2002). Salt allocation during leaf development and leaf fall in mangroves. *Trees* 16: 112-119. doi: 10.1007/s00468-001-0153-3
- Deng Y, Li J, Wu S, Zhu Y, Chen Y et al. (2006). Integrated nr database in protein annotation system and its localization. *Computer Engineering* 32: 71-77 (in Chinese with an abstract in English). doi: 10.1109/INFOCOM.2006.241
- Dubouzet J G, Sakuma Y, Ito Y, Kasuga M, Dubouzet E G et al. (2003). *OsDREB* genes in rice, *Oryza sativa* L., encode transcription activators that function in drought, high salt and cold responsive gene expression. *The Plant Journal* 33: 751-763. doi: 10.1046/j.1365-313X.2003.01661.x
- Forde BG, Lea PJ (2007). Glutamate in plants: metabolism, regulation, and signaling. *Journal of Experimental Botany* 58: 2339-2358. doi: 10.1093/jxb/erm121
- Gill SS, Tuteja N (2010). Reactive oxygen species and antioxidant machinery in abiotic stress tolerance in crop plants. *Plant Physiology and Biochemistry* 48: 909-930. doi: 10.1016/j.plaphy.2010.08.016
- Grabherr MG, Haas BJ, Yassour M, Levin JZ, Thompson, DA et al. (2011). Trinity: reconstructing a full-length transcriptome without a genome from RNA-Seq data. *Nature Biotechnology* 29: 644-652. doi: 10.1038/nbt.1883
- Guo H, Ecker JR (2004). The ethylene signaling pathway: new insights. *Current Opinion in Plant Biology* 7: 40-49. doi: 10.1016/j.pbi.2003.11.011
- Guo W, Wu H, Zhang Z, Yang C, Hu L et al. (2017). Comparative analysis of transcriptomes in Rhizophoraceae provides insights into the origin and adaptive evolution of mangrove plants in intertidal environments. *Frontiers in Plant Science* 8: 795. doi: 10.3389/fpls.2017.00795
- Guo Y, Huang C, Xie Y, Song F, Zhou X (2010). A tomato glutaredoxin gene *SlGRX1* regulates plant responses to oxidative, drought and salt stresses. *Planta* 232: 1499-1509. doi: 10.1007/s00425-010-1271-1
- Guri ASAF (1983). Variation in glutathione and ascorbic acid content among selected cultivars of *Phaseolus vulgaris* prior to and after exposure to ozone. *Revue Canadienne De Phytotechnie* 63: 10966-10974. doi: 10.4141/cjps83-090
- Halliwell B, Foyer CH (1978). Properties and physiological function of a glutathione reductase purified from spinach leaves by affinity chromatography. *Planta* 139: 9-17. doi: 10.2307/23373245
- Holmgren F, Alkhalfioui F, Yano H, Vensel W H, Hurkman W J et al. (2009). Thioredoxintargets in plants: the first 30 years. *Journal of Proteomics* 72: 452-474. doi: 10.1016/j.jprot.2008.12.002
- Huang Y, Li H, Gupta R, Morris P C, Luan S et al. (2000). AtMPK4, an Arabidopsis homolog of mitogen-activated protein kinase, is activated in vitro by AtMEK1 through threonine phosphorylation. *Plant Physiology* 122: 1301-1310. doi: 10.1104/pp.122.4.1301

- Hwang I, Chen HC, Sheen J (2002). Two-component signal transduction pathways in Arabidopsis. *Plant Physiology* 129: 500-515. doi: 10.1104/pp.005504
- Hyland K, Voisin E, Banoun H, Auclair C (1983). Superoxide dismutase assay using alkaline dimethylsulfoxide as superoxide anion-generating system, *Analytical Biochemistry* 135: 280-287. doi: 10.1016/0003-2697(83)90684-X
- Jordon-Thaden IE, Chanderbali AS, Gitzendanner MA, Soltis DE (2015). Modified CTAB and TRIzol protocols improve RNA extraction from chemically complex Embryophyta. *Application in Plant Science* 3: a1400105. doi: 10.3732/apps.1400105
- Kanehisa M, Araki M, Goto S, Hattori M, Hirakawa M et al. (2008). KEGG for linking genomes to life and the environment. *Nucleic Acids Research* 36: 480-484. doi: 10.1093/nar/gkm882
- Kekulandara DN, Nagi S, Seo H, Chow CS, Ahn YH (2018). Redox-inactive peptide disrupting trx1-ask1 interaction for selective activation of stress signaling, *Biochemistry* 57: 772-780. doi: 10.1021/acs.biochem.7b01083
- Kiegerl S, Cardinale F, Siligan C, Gross A, Baudouin E et al. (2000). SIMKK, a mitogen-activated protein kinase (MAPK) kinase, is a specific activator of the salt stress-induced MAPK, SIMK. *The Plant Cell* 12: 2247-2258. doi: 10.2307/3871118
- Krishnamurthy P, Mohanty B, Wijaya E (2017). Transcriptomics analysis of salt stress tolerance in the roots of the mangrove *Avicennia officinalis*. *Scientific Reports* 7: 10031. doi: 10.1038/s41598-017-10730-2
- Law M Y, Charles S A, Halliwell B (1983). Glutathione and ascorbic acid in spinach (*Spinacia oleracea*) chloroplasts. The effect of hydrogen peroxide and of paraquat. *Biochemical Journal* 210: 899-903. doi: 10.1042/bj2100899
- Lei G, Shen M, Li ZG, Zhang B, Duan KX et al. (2011). EIN2 regulates salt stress response and interacts with a MA3 domain-containing protein ECIP1 in Arabidopsis. *Plant, Cell & Environment* 34: 1678-1692. doi: 10.1111/j.1365-3040.2011.02363.x
- Liang S, Fang L, Zhou R, Tang T, Deng S et al. (2012). Transcriptional homeostasis of a mangrove species, *Ceriops tagal*, in saline environments, as revealed by microarray analysis. *PLoS ONE* 7: e36499. doi: 10.1371/journal.pone.0036499
- Livak KJ, Schmittgen TD (2001). Analysis of relative gene expression data using real-time quantitative PCR and the $2^{-\Delta\Delta CT}$ method. *Methods* 25: 402-408. doi: 10.1006/meth.2001.1262
- Lü XM, Yang YF, Lu XY, Jin J, Fan XM (2016). Effects of NaCl stress on the AsA-GSH cycle in sour jujube seedlings. *Plant Physiology Journal* 52: 736-744 (in Chinese with an abstract in English). doi: 10.13592/j.cnki.ppj.2015.0706
- Mishra A, Tanna B (2017). Halophytes: potential resources for salt stress tolerance genes and promoters. *Frontiers in Plant Science* 8: 829. doi: 10.3389/fpls.2017.00829
- Mittler R (2002). Oxidative stress, antioxidants and stress tolerance. *Trends in Plant Science* 7: 405-410. doi: 10.1016/S1360-1385(02)02312-9
- Miyama M, Tada Y (2008). Transcriptional and physiological study of the response of Burma mangrove (*Bruguiera gymnorhiza*) to salt and osmotic stress. *Plant Molecular Biology* 68: 119-129. doi: 10.1007/s11103-008-9356-y
- Mortazavi A, Williams BA, McCue K, Schaeffer L, Wold B (2008). Mapping and quantifying mammalian transcriptomes by RNA-Seq. *Nature Methods* 5: 621-628. doi: 10.1038/nmeth.1226
- Munns R (2002). Comparative physiology of salt and water stress. *Plant, Cell & Environment* 25: 239-250. doi: 10.1046/j.0016-8025.2001.00808.x
- Nakano Y, Asada K (1981). Hydrogen peroxide is scavenged by ascorbate-specific peroxidase in spinach chloroplasts. *Plant and Cell Physiology* 22: 867-880. doi: 10.1093/oxfordjournals.pcp.a076232
- Patterson BD, MacRae EA, Ferguson IB (1984a). Estimation of hydrogen peroxide in plant extracts using titanium (IV). *Analytical Biochemistry* 139: 487-492. doi: 10.1016/0003-2697(84)90039-3
- Patterson BD, Payne LA, Chen YZ, Graham D (1984b). An inhibitor of catalase induced by cold in chilling-sensitive plants. *Plant Physiology* 76: 1014-1018. doi: 10.2307/4269048
- Rouhier N, Gelhaye E, Jacquot JP (2002). Exploring the active site of plant glutaredoxin by site-directed mutagenesis. *FEBS Letters* 511: 145-149. doi: 10.1016/s0014-5793(01)03302-6
- Roy S J, Negrão S, Tester M (2014). Salt resistant crop plants. *Current Opinion in Biotechnology* 26: 115-124. doi: 10.1016/j.copbio.2013.12.004
- Saradhi PP, Mohanty P (1993). Proline in relation to free radical production in seedlings of *Brassica juncea* raised under sodium chloride stress. *Plant Soil* 155: 497-500. doi: 10.1007/bf00025092
- Seki M, Narusaka M, Ishida J, Nanjo T, Fujita M (2002). Monitoring the expression profiles of 7000 Arabidopsis genes under drought, cold and high-salinity stresses using a full-length cDNA microarray. *Plant Journal* 31: 279-292. doi: 10.1046/j.1365-313X.2002.01359.x
- Sharma R, Priya P, Jain M (2013). Modified expression of an auxin-responsive rice CC-type glutaredoxin gene affects multiple abiotic stress responses. *Planta* 238: 871-884. doi: 10.1007/s00425-013-1940-y
- Szabados L, Savouré A (2010). Proline: a multifunctional amino acid. *Trends in Plant Science* 15: 89-97. doi: 10.1016/j.tplants.2009.11.009
- Tatusov RL, Galperin MY, Natale DA, Koonin EV. (2000). The COG database: a tool for genome-scale analysis of protein functions and evolution. *Nucleic Acids Research* 28: 33-36. doi: 10.1093/nar/28.1.33
- Trapnell C, Pachter L, Salzberg SL (2009). TopHat: discovering splice junctions with RNA-Seq. *Bioinformatics* 25: 1105-1111. doi: 10.1093/bioinformatics/btp120
- Walia H, Wilson C, Zeng L, Ismail AM, Condamine P et al. (2007). Genome-wide transcriptional analysis of salinity stressed japonica and indica rice genotypes during panicle initiation stage. *Plant Molecular Biology* 63: 609-623. doi: 10.1007/s11103-006-9112-0

- Wang AG, Luo GH (1990). Quantitative relation between the reaction of hydroxylamine and superoxide anion radicals in plants. *Plant Physiology Communications* 84: 2895-2898. doi: 10.1021/ja00874a010 (in Chinese with an abstract in English)
- Wang L, Pan D, Lv X, Cheng C-L, Li J et al. (2016). A multilevel investigation to discover why *Kandelia candel* thrives in high salinity. *Plant, Cell & Environment* 39: 2486-2497. doi: 10.1111/pce.12804
- Wang L, Pan D, Li J, Tan F, Hoffmann-Benning S et al. (2015). Proteomic analysis of changes in the *Kandelia candel* chloroplast proteins reveals pathways associated with salt tolerance. *Plant Science* 231: 159-172. doi: 10.1016/j.plantsci.2014.11.013
- Wang NN, Shih M C, Li N (2005). The GUS reporter-aided analysis of the promoter activities of *Arabidopsis* ACC synthase genes *AtACS4*, *AtACS5*, and *AtACS7* induced by hormones and stresses. *Journal of Experimental Botany* 56: 909-920. doi: 10.1093/jxb/eri083
- Yang F, Tan H, Zhou Y, Lin X, Zhang S. (2011). High-Quality RNA Preparation from *Rhodosporidium toruloides* and cDNA Library Construction Therewith. *Molecular Biotechnology*, 47: 144-151. doi: 10.1007/s12033-010-9322-1
- Yao D, Zhang X, Zhao X, Liu C, Wang C et al. (2011). Transcriptome analysis reveals salt-stress-regulated biological processes and key pathways in roots of cotton (*Gossypium hirsutum* L.). *Genomics* 98: 47-55. doi: 10.1016/j.ygeno.2011.04.007
- Yasumoto E, Adachi K, Kato M, Sano H, Sasamoto H et al. (1999). Uptake of inorganic ions and compatible solutes in cultured mangrove cells during salt stress. *In Vitro Cellular & Developmental Biology-Plant* 35: 82-85. doi: 10.2307/4293165
- Ye J, Fang L, Zheng H, Zhang Y, Chen J et al. (2006). WEGO: a web tool for plotting GO annotations. *Nucleic Acids Research* 34: 293-297. doi: 10.1093/nar/gkl031
- Yu J, Chen S, Zhao Q, Wang T, Yang C et al. (2011). Physiological and proteomic analysis of salinity tolerance in *Puccinellia tenuiflora*. *Journal of Proteome Research* 10: 3852-3870. doi: 10.1021/pr101102p

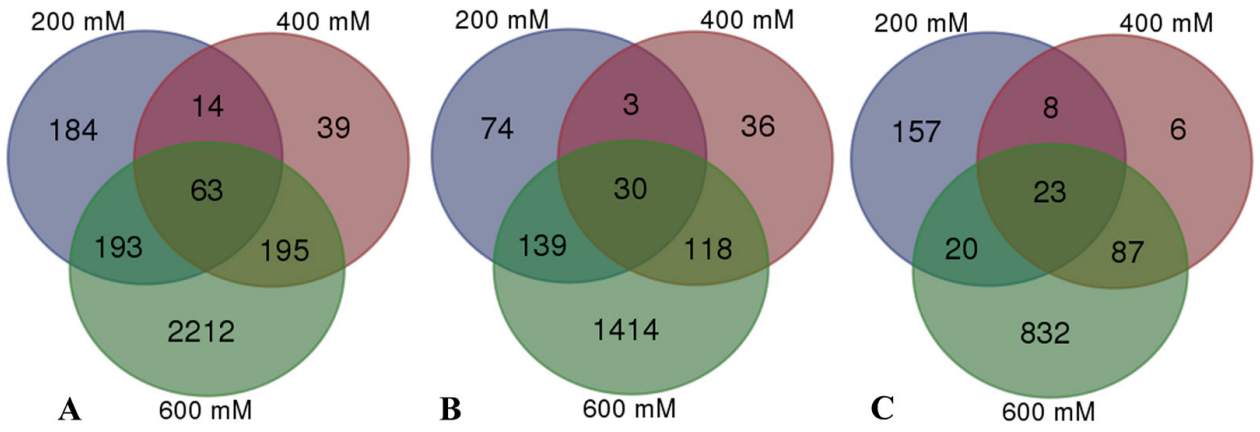


Figure S1. Venn diagrams of distinct and common differentially expressed genes in *K. candel* roots under salt stress. A: Total DEGs; B: Upregulated DEGs; C: Downregulated DEGs.

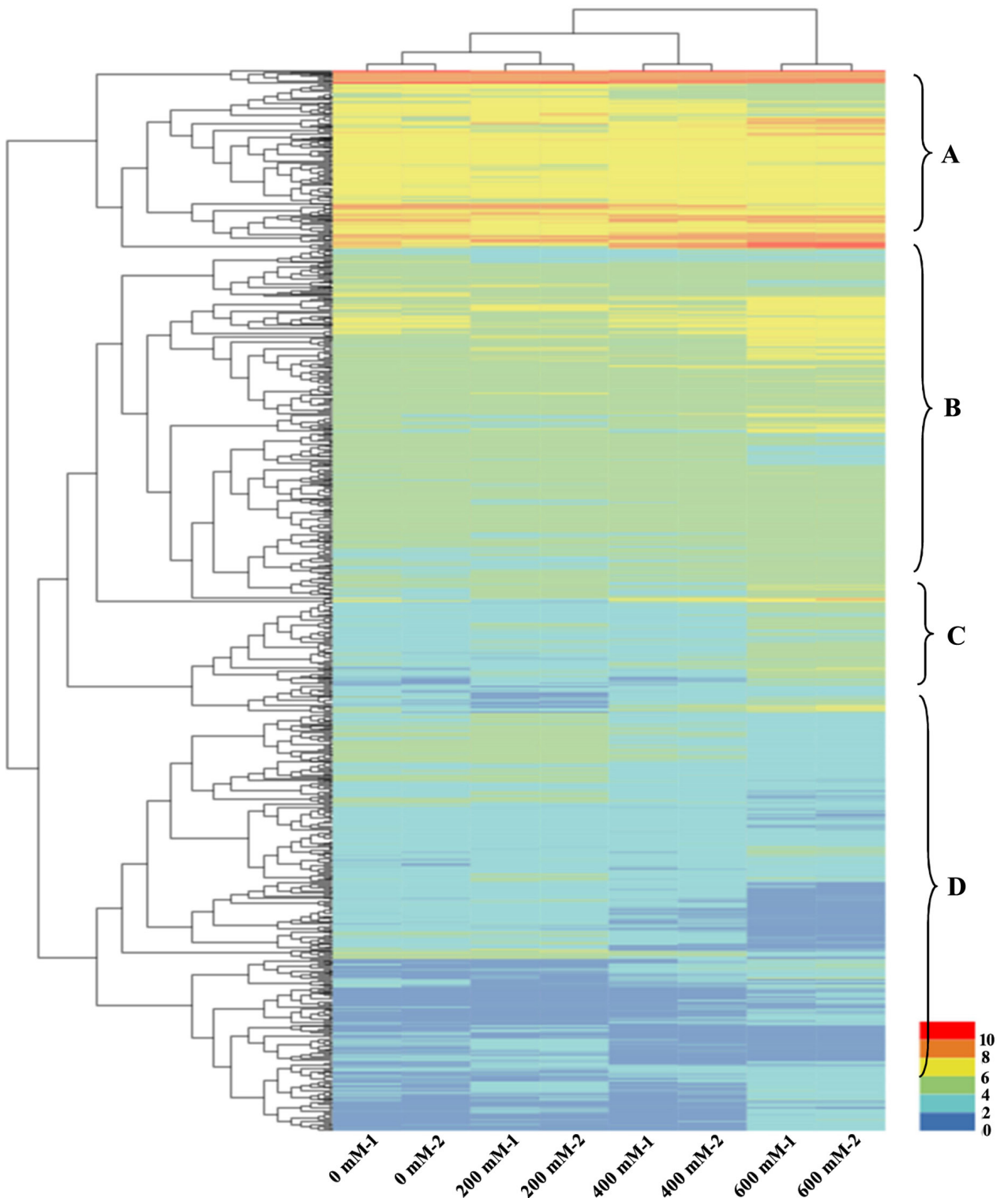


Figure S2. Hierarchical clustering analysis of differentially expressed genes under salt stress of *K. candel* roots. The numbers 0-10 indicates the signal ratios which are shown in a red-green color scale, where red represents upregulation and green represents downregulation. Each column (0 mM-1, 0 mM-2, 200 mM-1, 200 mM-2, 400 mM-1, 400 mM-2, 600 mM-1, 600 mM-2) represents the mean expression value of the RNA-Seq obtained from two biological replicates and each row represents a differentially expressed genes (DEGs). A, B, C and D represent four differential trends of DEGs respectively, among which A represents all upregulated genes, B represents most upregulated genes, C represents most downregulated genes, and D represents all downregulated genes.

